

## Effect of Hypothermia on the Thalamocortical Function in the Rat Model

Anil Maybhathe, PhD, *Member, IEEE*, Cheng Chen, BS, *Student Member, IEEE*,  
Nitish V. Thakor, PhD, *Fellow, IEEE*, Xiaofeng Jia, MD, PhD

**Abstract** — Neuroprotective effects of hypothermia are well documented in many injuries of the central nervous system in animal models as well as clinical studies. However, the underlying mechanisms are not fully understood. An important yet unexplored background issue is the effect of hypothermic cooling on the regional functionality of the healthy CNS. In a pilot study with the rat model, we seek to characterize the effect of moderate bodily cooling on the thalamo-cortical (T-C) function. Multiunit activity (MUA) and local field potentials (LFPs) were recorded from the thalamus (VPL nucleus) and the somatosensory cortex (S1) for normothermic, mild hypothermic and mild hyperthermic conditions in healthy rats and the thalamo-cortical dynamics was characterized with Granger Causal Interaction (GCI). The GCI indicated that the thalamic driving of the cortical activity significantly increases in strength with bodily cooling and weakens with mild heating. These results could have important implications towards understanding of hypothermia.

### I. INTRODUCTION

Neuroprotection with hypothermia has recently attracted a lot of attention from basic scientists [1], translational researchers [2, 3] and clinicians [4, 5]. The beneficial effects of hypothermia have been explored extensively in pathologies like neurological injury from hypoxic-ischemia [6, 7], spinal cord injury [8], traumatic brain injury [9], stroke [10] and coma [11], etc. A common factor in all these CNS injuries is a post-acute secondary cascade of molecular events, which leads to inflammation, widespread neuronal degeneration that eventually results into a poor outcome. In order to understand basic electrophysiological underpinnings of hypothermia based therapies, it is essential to study the effects of temperature changes on the regional functions and interdependencies in the CNS. We have recently explored the effect of induced hypothermia on the EEG and somatosensory evoked potentials (SSEPs) of an uninjured brain in a rodent model [12]. Here, we focus on how temperature modulation affects the coupled functionality of the thalamocortical circuits in a rat model. Previous studies have showed that the synchronous thalamocortical activity plays a critical role

in maintaining the conscious state [13], arousal from sleep [14], and arousal from coma during recovery from injury [15, 16]. Thus, it is reasonable to hypothesize that the reported beneficial effects of hypothermia may entail an effect on the thalamocortical functionality and we aim to study these changes in a rat model.

Based on the anatomy of the thalamocortical nuclei and where they send their projections [17], we focus on a single, easily accessible area of the thalamus, the ventral posterolateral (VPL) nucleus that corresponds to the somatosensory cortex (S1). We recorded the MUA and the LFPs simultaneously from the VPL nucleus and the somatosensory cortex (S1 Layer IV-V, Forelimb). For analysis, we employed a well-established powerful method, the Granger Causality Analysis to uncover the direction and extent of the information flow from the two regions [18]. This was adopted to define the Granger Causal Interaction (GCI) matrix to characterize the strength of dynamical driving from the thalamus to the cortex and vice versa. Finally, the GCI was assessed in a rat model with normothermia ( $37\pm 0.5^\circ\text{C}$ ); mild hypothermia ( $33\pm 0.5^\circ\text{C}$ ) and mild hyperthermia ( $39\pm 0.5^\circ\text{C}$ ).

### II. METHODS

#### A. Experimental Procedures

Adult male Wistar rats (300-350gms; Charles River Laboratories, Germantown, MD) were used. The animals were housed individually in cages and had free access to food and water. All the procedures were approved by the Institutional Animal Care and Use Committee at the Johns Hopkins University.

Briefly, after initial preparations with anesthesia, and stereotaxic fixing (Kopf, Model 957, Tujunga, CA), the rat was subjected to a controlled flow of the anesthetic gas (1.5% halothane) via a tight-fitting facemask and placed on a heat pad (TCAT-2 Temp Controller, Physitemp, Clifton, NJ). The controller's temperature probe was advanced into the rectum to continuously monitor the body temperature through the recording session. A local anesthetic of 2% Lidocaine HCl (Abbott Laboratories, North Chicago, IL) was injected under the skin, and an incision was made along the midline. The cranium bone was cleaned by removing the tissue under the skin.

Under a surgical microscope, a standard dental drill (Fine Science Tools, North Vancouver, BC, Canada) was used to drill two small holes (located directly above the VPL and S1FL areas as per Ref. [19]) in the skull without puncturing the dura. Using the standard anatomical atlas coordinates two pairs of two-channel tungsten micro-electrodes (FHC, Bowdoinham, ME) were advanced

Research supported by the National Institute of Health (grant#1RO1HL7156) and the American Heart Association (grant#09SDG2110140).

A. Maybhathe (anil@jhmi.edu), C. Chen (cchen155@jhu.edu), N. V. Thakor (nitith@jhu.edu) and X. Jia (xjia1@jhmi.edu) are all with the Department of Biomedical Engineering, Johns Hopkins University, 720 Rutland Avenue, Traylor Building, Room 710-C, Baltimore, MD 21205. Corresponding Author: Anil Maybhathe; Phone: (443) 287 6341; email: anil@jhmi.edu

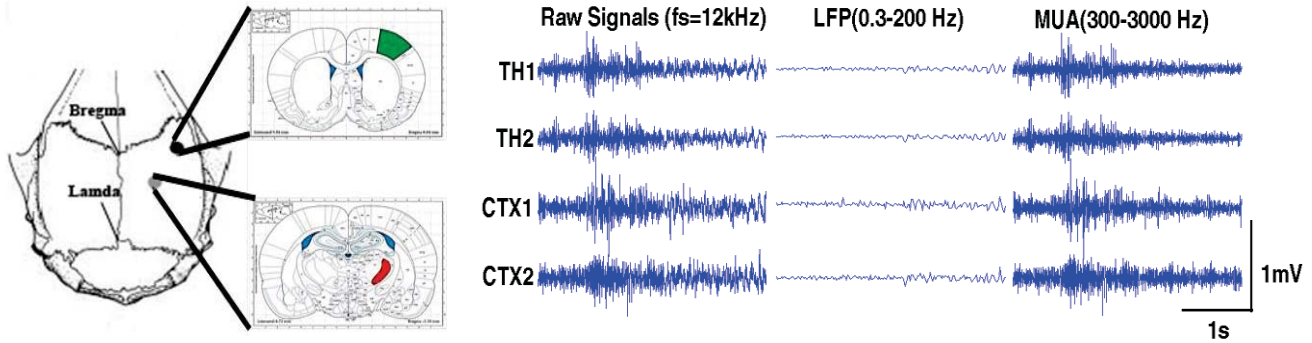


**Figure 1.** Left: Schematic for the electrode placements on the dorsal view of the rat skull shown along with coronal cross-section as per the anatomical atlas [19]; marking the somatosensory cortical region for forelimb (S1FL, Green) and the thalamic ventral postero-lateral nucleus (VPL). Right: The recorded combined signal from the four channels, before and after separation into the local field potentials (LFPs) and multi-unit activity (MUA).

to the layer IV-V of the somatosensory cortex and the VPL nucleus of the thalamus.

After the rats were stabilized at normothermic temperature ( $37 \pm 0.5^\circ\text{C}$ ), the thalamocortical MUA and LFPs were recorded for 10mins. The rat was then cooled down to the hypothermic range ( $32\text{--}34^\circ\text{C}$ ) by external systemic cooling using a fan and alcohol-water mist spray within 15 minutes [20, 21].

The temperature was allowed to stabilize within the hypothermic range prior to recording to reach a thermal steady state [22]. Finally, the rats were gradually warmed up to the hyperthermic range ( $39 \pm 0.5^\circ\text{C}$ ) using an infra-red lamp (Thermalet TH-5, model 6333, Physitemp, NJ, USA), and signals were recorded for 10mins after stabilization of temperature ( $39 \pm 0.5^\circ\text{C}$ ).

The heart rate and the blood pressure were monitored throughout. MUA and LFP Signals were digitally acquired at the sampling rate of 6.1 kHz using TDT System3 (Tucker-Davis Technologies, Alachua, FL); filtered (0.3-3kHz) and stored for further analysis. Finally, the rat was released from stereotaxic frame after the recording, and was euthanized using intracardiac injection of overdosed KCL.

### B. Post-experimental Data Analysis

The acquired raw signal was notch filtered to remove the 60Hz noise, band-pass filtered with 0.3-200Hz for LFP and band-pass filtered with 300-3000 Hz for MUA. The LFP signals were subjected to the granger causality analysis to compute the GCI matrix, and the MUA signals representing the neural spikes were used to calculate the inter-spike interval histograms.

The Granger causality test is a statistical hypothesis test for determining whether one time series is useful in forecasting another. Ganger causality [23] is defined as follows: for two simultaneously recorded signals  $X_1, X_2$ , if the future values of  $X_2$  can be predicted better by incorporating the past information from  $X_1$  than just using the information from  $X_2$ , then it can be said that  $X_1$  is causally affecting  $X_2$ . Therefore it could be said that the underlying system generating the signal  $X_1$  is *dynamically driving*  $X_2$ . In lieu of the knowledge of underlying causation,

Granger causality is one of the most powerful definitions of observable causality.

In the context of our animal model, suppose the thalamic and cortical time series recorded can be represented by two discrete random variables  $X_1(t), X_2(t)$  which can be modeled by the bivariate autoregressive processes [24, 25]:

$$X_1(t) = \sum_{i=1}^p A_{11}(i)X_1(t-i) + \sum_{i=1}^p A_{12}(i)X_2(t-i) + E_1(t) \quad (1)$$

$$X_2(t) = \sum_{i=1}^p A_{21}(i)X_1(t-i) + \sum_{i=1}^p A_{22}(i)X_2(t-i) + E_2(t), \quad (2)$$

where  $E_1(t)$  and  $E_2(t)$  denote the variance of the prediction error. If  $E_1$  (or  $E_2$ ) become smaller by including  $X_2$  (or  $X_1$ ) term  $n(1)$  (or  $(2)$ ), then  $X_2$  (or  $X_1$ ) is the causal to  $X_1$  (or  $X_2$ ). Equation (1) and (2) can be transformed to frequency domain using Fourier transform, that is,

$$\begin{pmatrix} X_1(f) \\ X_2(f) \end{pmatrix} = \begin{pmatrix} H_{11}(f) & H_{12}(f) \\ H_{21}(f) & H_{22}(f) \end{pmatrix} \begin{pmatrix} E_1(f) \\ E_2(f) \end{pmatrix} \quad (3)$$

The spectral matrix is calculated using following equation:

$$S(f) = H(f)ZH^*(f), \quad (4)$$

where  $Z$  is the *covariance matrix* of residual error and the asterisk denotes matrix transpose with complex conjugation.

The thalamocortical driving strength from channel  $k$  to channel  $l$  in frequency domain can be defined as the Granger Causal Interaction (GSI), denoted by  $I_{k \rightarrow l}$ , is given by,

$$I_{k \rightarrow l}(f) = \frac{(Z_{kk} - \frac{Z_{lk}^2}{Z_{ll}})|H_{lk}(f)|^2}{S_{ll}(f)} \quad (5)$$

## III. RESULTS

We recorded a total of 4 channels: 2 from the VPL nucleus of the thalamus (labeled TH1, TH2) and 2 from the S1FL area (labeled CTX1, CTX2). The recorded signal was a very

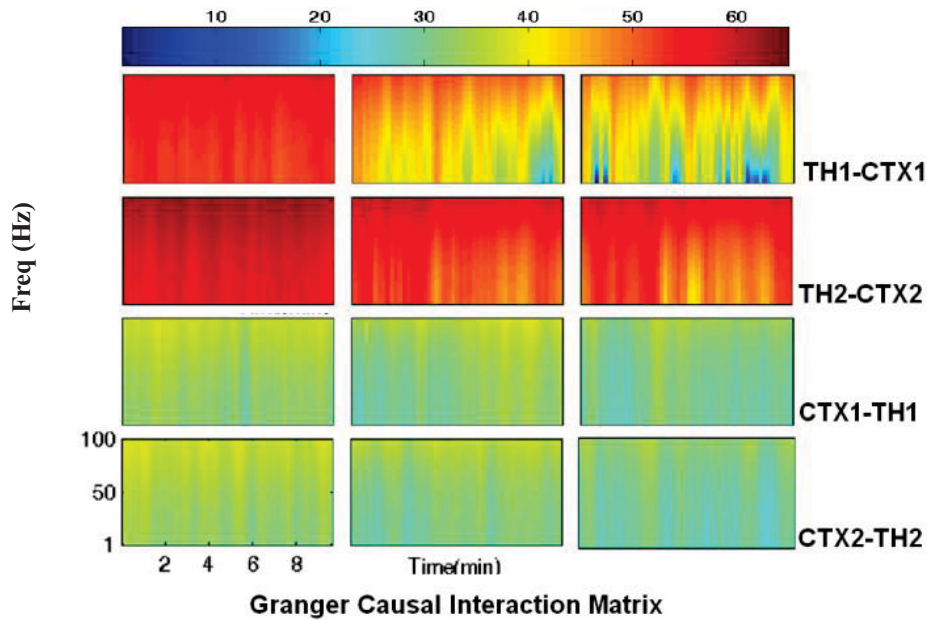


**Figure 2:** The Granger causal interaction (GCI) matrices are shown in the time-frequency domain for four labeled pairs of thalamic and cortical electrodes. The cross-channel matrices are not shown for brevity and were similar to the ones shown. The left most column corresponds to mild hypothermia; the middle column corresponds to normothermia and the right most column corresponds to mild hyperthermia. These results suggest that the thalamocortical driving strength underwent a marked increase for the hypothermic interval while did not weaken during hyperthermia. All through the three phases, the reverse driving did not change markedly.

wide-band signal sampled at 6.1kHz. This was separated as described in methods into the LFP and MUA.

**Figure 1** (right panel) shows an example trace of the recorded 4-ch signal, along with the separated LFP (the low frequency component 0.3-200Hz) and the MUA (high frequency component 300-3000Hz). The algorithm was implemented in MATLAB (Mathworks, Natick, MA) to calculate the GCI matrix between each pair of the 4 electrodes. **Figure 2** shows the color coded GCI plotted between 1-100Hz for four such pairs, for the normothermic, hypothermic and hyperthermic phase of the recording. It is evident from this figure that the cooling led to a stronger driving from the thalamus throughout the spectral components, while a mild warming led to a slight but insignificant weakening of this drive. The reverse causal influence, from the cortex to the thalamus was similar in all the three phases.

Interestingly as shown in **Figure 3**, the spiking activity itself, as assessed from the MUA signal and computing the inter-spike interval histogram, actually decreased slightly in hypothermic phase as compared to normothermic; and did not show a marked change during the mild hyperthermia.

#### IV. DISCUSSION

In this study, we measured the changes of thalamocortical function during hypothermic cooling and mild hyperthermic warming. Results based on Granger causality analysis reflect that the causal relationship between thalamus and cortex is markedly increased in the cooling period.

It should be noted that despite the name, Granger causality is an estimate and cannot imply true causality. If

two processes are driven by a common third process with different lags, one might still accept the alternative hypothesis of Granger causality. Yet, manipulation of one of the variables would not change the other. Furthermore, the Granger test can produce misleading results when the true relationship involves higher than two dimensional underlying dynamics. A similar test involving more variables can be applied with vector auto-regression.

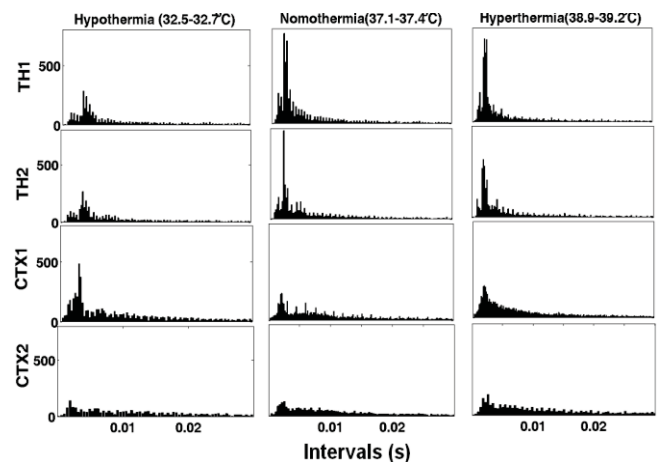


**Figure 3:** Inter-spike Interval histograms for the four channels recorded during hypothermia (left), normothermia (middle), mild hyperthermia (right) from the thalamus and S1 cortex of an anesthetized rat. There was no notable difference in the normothermia and mildly hyperthermic firing rates. There was a marked decrease during hypothermia in the thalamic activity and a slight increase in the cortical activity. Yet the strength of driving from thalamus to cortex was drastically more during hypothermia.



## V. CONCLUSION

Our preliminary results suggest that the thalamus leads an important role in maintaining network connectivity to cortex. It may drive the cortical activity during the hypothermic treatment and thus perhaps contributes to the neuroprotection during the recovery from an injury. Further validation through more extensive simultaneous intra-cortical recording of spike activity from neurons in thalamus and cortex will be needed to confirm this research and better understand the mechanisms. The results, when further validated with more experiment, could potentially shed light on the region-specific activities that underlie the hypothermic treatment and thus in future, help improve the intervention protocols.

## REFERENCES

1. Yenari, M.A. and H.S. Han, Neuroprotective mechanisms of hypothermia in brain ischaemia. *Nat Rev Neurosci*, 2012. 13(4): p. 267-278.
2. Maybhate, A., C. Hu, F.A. Bazley, Q. Yu, N.V. Thakor, C.L. Kerr, and A.H. All, Potential long-term benefits of acute hypothermia after spinal cord injury: Assessments with somatosensory-evoked potentials\*. *Critical Care Medicine*, 2012. 40(2): p. 573.
3. Kwon, B.K., L.H. Sekhon, and M.G. Fehlings, Emerging repair, regeneration, and translational research advances for spinal cord injury. *Spine*, 2010. 35(21S): p. S263.
4. Dietrich, W.D., Therapeutic hypothermia for acute severe spinal cord injury: Ready to start large clinical trials?\*. *Critical Care Medicine*, 2012. 40(2): p. 691.
5. Shah, P.S. Hypothermia: a systematic review and meta-analysis of clinical trials. 2010: Elsevier.
6. Madhok, J., A. Maybhate, W. Xiong, M.A. Koenig, R.G. Geocadin, X. Jia, and N.V. Thakor, Quantitative assessment of somatosensory-evoked potentials after cardiac arrest in rats: Prognostication of functional outcomes. *Critical Care Medicine*, 2010. 38(8): p. 1709.
7. Kang, X., X. Jia, R.G. Geocadin, N.V. Thakor, and A. Maybhate, Multiscale entropy analysis of EEG for assessment of post-cardiac arrest neurological recovery under hypothermia in rats. *Biomedical Engineering, IEEE Transactions on*, 2009. 56(4): p. 1023-1031.
8. Levi, A.D., G. Casella, B.A. Green, W.D. Dietrich, S. Vanni, J. Jagid, and M.Y. Wang, Clinical outcomes using modest intravascular hypothermia after acute cervical spinal cord injury. *Neurosurgery*, 2010. 66(4): p. 670.
9. Clifton, G.L., A Review of Clinical Trials of Hypothermia Treatment for Severe Traumatic Brain Injury. *Therapeutic Hypothermia and Temperature Management*, 2011.
10. Groysman, L.I., B.A. Emanuel, M.A. Kim-Tenser, G.Y. Sung, and W.J. Mack, Therapeutic hypothermia in acute ischemic stroke. *Neurosurgical Focus*, 2011. 30(6): p. 17.
11. Bernard, S.A., T.W. Gray, M.D. Buist, B.M. Jones, W. Silvester, G. Gutteridge, and K. Smith, Treatment of comatose survivors of out-of-hospital cardiac arrest with induced hypothermia. *New England Journal of Medicine*, 2002. 346(8): p. 557-563.
12. Madhok, J., D. Wu, W. Xiong, R.G. Geocadin, and X. Jia, Hypothermia Amplifies Somatosensory-evoked Potentials in Uninjured Rats. *Journal of Neurosurgical Anesthesiology*, 2012.
13. Llinás, R., U. Ribary, D. Contreras, and C. Pedroarena, The neuronal basis for consciousness. *Philosophical Transactions of the Royal Society of London. Series B: Biological Sciences*, 1998. 353(1377): p. 1841-1849.
14. McCormick, D.A. and T. Bal, Sleep and arousal: thalamocortical mechanisms. *Annual review of neuroscience*, 1997. 20(1): p. 185-215.
15. Laureys, S., M.E. Faymonville, A. Luxen, M. Lamy, G. Franck, and P. Maquet, Restoration of thalamocortical connectivity after recovery from persistent vegetative state. *The Lancet*, 2000. 355(9217): p. 1790-1791.
16. Schiff, N.D. and F. Plum, The role of arousal and "gating" systems in the neurology of impaired consciousness. *Journal of Clinical Neurophysiology*, 2000. 17(5): p. 438.
17. Diamond, M.E., M. Armstrong-James, and F.F. Ebner, Somatic sensory responses in the rostral sector of the posterior group (POm) and in the ventral posterior medial nucleus (VPM) of the rat thalamus. *The Journal of comparative neurology*, 1992. 318(4): p. 462-476.
18. Bressler, S.L., C.G. Richter, Y. Chen, and M. Ding, Cortical functional network organization from autoregressive modeling of local field potential oscillations. *Statistics in medicine*, 2007. 26(21): p. 3875-3885.
19. Paxinos, G. and C. Watson, *The Rat Brain in Stereotaxic Coordinates: Hard Cover Edition*. 5 ed. 2007, San Diego, CA: Elsevier Academic Press Inc.
20. Jia, X., M.A. Koenig, R. Nickl, G. Zhen, N.V. Thakor, and R.G. Geocadin, Early electrophysiologic markers predict functional outcome associated with temperature manipulation after cardiac arrest in rats. *Critical Care Medicine*, 2008. 36(6): p. 1909.
21. Jia, X., M.A. Koenig, H.C. Shin, G. Zhen, C.A. Pardo, D.F. Hanley, N.V. Thakor, and R.G. Geocadin, Improving neurological outcomes post-cardiac arrest in a rat model: immediate hypothermia and quantitative EEG monitoring. *Resuscitation*, 2008. 76(3): p. 431-442.
22. Geocadin, R.G., M.A. Koenig, X. Jia, R.D. Stevens, and M.A. Peberdy, Management of brain injury after resuscitation from cardiac arrest. *Neurologic clinics*, 2008. 26(2): p. 487-506.
23. Granger, C.W.J., Investigating causal relations by econometric models and cross-spectral methods. *Econometrica: Journal of the Econometric Society*, 1969: p. 424-438.
24. Bressler, S.L. and A.K. Seth, Wiener-Granger Causality: A well established methodology. *Neuroimage*, 2011. 58(2): p. 323-329.
25. Seth, A.K., A MATLAB toolbox for Granger causal connectivity analysis. *Journal of neuroscience methods*, 2010. 186(2): p. 262-273.